A&A 475, 1185–1194 (2007)
DOI: 10.1051/0004-6361:20077582

Astronomy & Astrophysics

Nulling interferometry: performance comparison between Antarctica and other ground-based sites

O. Absil[1,2,⋆], V. Coudé du Foresto[3], M. Barillot[4], and M. R. Swain[5]

[1] LAOG, Université Joseph Fourier, CNRS, 414 rue de la Piscine, 38400 Grenoble, France
e-mail: olivier.absil@obs.ujf-grenoble.fr
[2] Institut d'Astrophysique et de Géophysique, Université de Liège, 17 Allée du Six Août, 4000 Liège, Belgium
[3] LESIA, Observatoire de Paris-Meudon, CNRS, 5 place Jules Janssen, 92195 Meudon, France
[4] Thales Alenia Space, 100 bd du Midi, 06156 Cannes La Bocca, France
[5] Jet Propulsion Laboratory, California Institute of Technology, 4800 Oak Grove Drive, Pasadena, CA 91109, USA

Received 2 April 2007 / Accepted 28 August 2007

ABSTRACT

Context. Detecting the presence of circumstellar dust around nearby solar-type main sequence stars is an important pre-requisite for the design of future life-finding space missions such as ESA's Darwin or NASA's Terrestrial Planet Finder (TPF). The high Antarctic plateau may provide appropriate conditions to perform such a survey from the ground.
Aims. We investigate the performance of a nulling interferometer optimised for the detection of exozodiacal discs at Dome C, on the high Antarctic plateau, and compare it to the expected performance of similar instruments at temperate sites.
Methods. Based on the currently available measurements of the atmospheric turbulence characteristics at Dome C, we adapt the GENIEsim software (Absil et al. 2006, A&A, 448, 787) to simulate the performance of a nulling interferometer on the high Antarctic plateau. To feed a realistic instrumental configuration into the simulator, we propose a conceptual design for ALADDIN, the Antarctic *L*-band Astrophysics Discovery Demonstrator for Interferometric Nulling. We assume that this instrument can be placed above the 30-m thick boundary layer, where most of the atmospheric turbulence originates.
Results. We show that an optimised nulling interferometer operating on a pair of 1-m class telescopes located 30 m above the ground could achieve a better sensitivity than a similar instrument working with two 8-m class telescopes at a temperate site such as Cerro Paranal. The detection of circumstellar discs about 20 times as dense as our local zodiacal cloud seems within reach for typical Darwin/TPF targets in an integration time of a few hours. Moreover, the exceptional turbulence conditions significantly relax the requirements on real-time control loops, which has favourable consequences on the feasibility of the nulling instrument.
Conclusions. The perspectives for high dynamic range, high angular resolution infrared astronomy on the high Antarctic plateau look very promising.

Key words. atmospheric effects – instrumentation: high angular resolution – techniques: interferometric – circumstellar matter

1. Introduction

Nulling interferometry is considered to be the technique that can enable the spectroscopic characterisation of the atmosphere of habitable extrasolar planets in the thermal infrared, where markers of biological activity have been identified (Kaltenegger et al. 2007). This is actually the objective of the Darwin and TPF-I missions studied by ESA and NASA, respectively (Fridlund 2004; Beichman et al. 1999). While the spectral domain (6−20 μm, where the atmosphere is mostly opaque) and required dynamic range ($\sim 10^7$) mandate a space interferometer to achieve this goal, a ground-based pathfinder might be needed to demonstrate the technique in an operational context, carry out precursor science, and therefore pave the way for space missions.

One of the main limitations of ground-based nulling interferometers is related to the influence of atmospheric turbulence. Active compensation of the harmful effects of turbulence requires real-time control systems to be designed with challenging requirements (Absil et al. 2006a, hereafter Paper I). The choice of a good astronomical site with (s)low turbulence is therefore of critical importance. In this respect, recent studies suggest that the high Antarctic plateau might be the best place on Earth to perform high angular resolution observations in the infrared domain, thanks to its very stable atmospheric conditions.

The Antarctic plateau has long been recognised as a high-quality site for observational astronomy, mainly in the context of sub-millimetric and infrared applications, for which the low temperature and low water vapour content bring a substantial gain in sensitivity. However, the only site that has been extensively used for astronomy so far is the South Pole, where high wind velocity causes poor turbulence conditions and thereby prevents high angular resolution applications in the near-infrared. The construction of the French-Italian Concordia station at Dome C (75°S, 123°E) has recently opened the path to new and exciting astronomical studies (Candidi & Lori 2003). Its main peculiarity with respect to the South Pole station is that it resides on a local summit of the plateau (3250 m), where katabatic winds have not yet acquired a significant velocity nor a large thickness by flowing down the slope of the plateau. For this reason, it is expected that Dome C could become the best accessible site on the continent, and, given its promising environmental characteristics, it is worthwhile to investigate its potential for a ground-based nulling interferometer.

⋆ Marie-Curie EIF Postdoctoral Fellow.

2. Mission definition

In order to provide a valid comparison with respect to a temperate site, we chose to study the potential of the Antarctic plateau in the context of a well specified mission, i.e., the ground-based Darwin demonstrator that has been identified and studied by ESA at the phase A level (Gondoin et al. 2004). In its original version, GENIE (Ground-based European Nulling Interferometer Experiment) is conceived as a focal instrument of the VLTI and its science objective is the study of exozodiacal dust around nearby solar-type stars like the Darwin targets. Indeed, our knowledge of the dust distribution in the first few AUs around solar-type stars is currently mostly limited to the observation of the solar zodiacal disc, a sparse structure of warm silicate grains 10 to 100 μm in diameter, which is the most luminous component of the solar system after the Sun. The presence of similar discs around the Darwin targets (exozodiacal discs) may represent a severe limitation to the Earth-like planet detection capabilities of this mission, as warm exozodiacal dust becomes the main source of noise if it is more than 20 times as dense as in the solar zodiacal disc (Beichman et al. 2006). Ongoing interferometric studies are indeed suggesting that dense exozodiacal discs may be more common than anticipated (Absil et al. 2006b; Di Folco et al. 2007). The prevalence of dust in the habitable zone around nearby solar-type stars must therefore be assessed before finalising the design of the Darwin mission.

Besides its scientific goals, the demonstrator also serves as a technology test bench to validate the operation of nulling interferometry on the sky.

3. Atmospheric parameters at Dome C

Several locations on the Antarctic plateau are expected to provide excellent atmospheric conditions for high-angular resolution astronomy. Because Dome C has been extensively characterised during the past years, it is taken as a reference site for the present study. It might well turn out in the future that other sites, such as Dome A or Dome F, are better suited than Dome C for the considered mission. One the one hand, the height of the turbulent ground layer might be thinner than at Dome C (Swain & Gallée 2006b), while on the other hand, free air seeing[1] could be somewhat smaller at Antarctic sites located closer to the centre of the polar vortex (Marks 2002).

3.1. Atmospheric turbulence

Intensive site characterisation at Dome C has been carried out since the austral summer 2002–03, with the deployment of several instruments (Aristidi et al. 2003; Lawrence et al. 2003). First, daytime seeing measurements with a Differential Image Motion Monitor (DIMM) were used to derive a median seeing value of 1.″2 (Aristidi et al. 2003). Later on, using a Multi-Aperture Scintillation Sensor (MASS) and a Sonic radar (SODAR) in automated mode during wintertime, Lawrence et al. (2004) reported a median seeing of 0.″27. The isoplanatic angle θ_0 and coherence time τ_0 were also derived from MASS measurements, with average values of 5.″7 and 7.9 msec respectively. For comparison, the corresponding values at Cerro Paranal are $\theta_0 = 2.''5$ and $\tau_0 = 3.3$ ms. These outstanding atmospheric conditions are however valid only above 30 m, as the SODAR measures the distribution of turbulence in an atmospheric layer comprised between 30 and 900 m above the ground, while the MASS is insensitive to seeing below about 500 m.

These first results suggest that most of the atmospheric turbulence is concentrated in a thin boundary layer, about 30 m thick. The simultaneous use of two DIMMs at different heights (3 m and 8 m above the ice surface) further confirms this fact, showing that half of the turbulence is concentrated into the first 5 m above the surface (Aristidi et al. 2005). A similar behaviour had already been reported at the South Pole, where SODAR measurements showed that turbulence was mostly confined to a boundary layer sitting below 270 m (Travouillon et al. 2003). This behaviour can be explained by the horizontal katabatic wind, whose altitude profile closely matches the turbulence profile.

In 2005, the first winter-over mission at Dome C has allowed DIMM measurements and balloon-borne thermal measurements to be obtained during the long Antarctic night. Preliminary results reported by Agabi et al. (2006) confirm the two-layered structure of atmospheric turbulence at Dome C. A 36-m thick surface layer is responsible for 87% of the turbulence, resulting in a total seeing of $1.''9 \pm 0.''5$, while the very stable free atmosphere has a median seeing of $0.''36 \pm 0.''19$ above 30 m. This value is remarkably similar to the median free air seeing of 0.″32 reported at South Pole by Marks et al. (1999).

3.2. Water vapour seeing

Another critical parameter for infrared observations is the water vapour content of the atmosphere. On one hand, it strongly influences the sky transparency as a function of wavelength, and on the other hand, its temporal fluctuations are an important source of noise for infrared observations. The water vapour content of the Antarctic atmosphere has been measured at South Pole by radiosonde, giving an exceptionally low average value of 250 μm during austral winter (Chamberlin et al. 1997; Bussmann et al. 2005), where temperate sites typically have a few millimetres of precipitable water vapour (*PWV*). This is mainly due to the extreme coldness of the air, with a ground-level temperature of about −61 °C (212 K) at the South Pole during winter[2], which induces a low saturation pressure for water vapour. The winter time *PWV* at Dome C is estimated to be between 160 μm (Lawrence 2004) and 350 μm (Swain & Gallée 2006a).

The very low water vapour content of the Dome C atmosphere has an important advantage in the context of high-precision infrared interferometry: longitudinal dispersion, created by the fluctuations of the water vapour column density above the telescopes (Colavita et al. 2004), is greatly reduced with respect to temperate sites. The standard deviation of *PWV* (σ_{PWV}) can be estimated at Dome C assuming that water vapour seeing follows the same statistics as the piston, as suggested by Lay (1997). In that case, the standard deviation of *PWV* fluctuation depends on the Fried parameter r_0 viz. $\sigma_{PWV} \propto r_0^{-5/6}$ according to Roddier (1981). Assuming that σ_{PWV} is also proportional to $\langle PWV \rangle$, the average *PWV* content, its value at Dome C can then be obtained by means of a comparison with the data obtained at temperate sites:

$$\sigma_{PWV}(\mathrm{DC}) = \frac{\langle PWV \rangle_{\mathrm{DC}}}{\langle PWV \rangle_i} \left(\frac{r_{0,\mathrm{DC}}}{r_{0,i}} \right)^{-5/6} \sigma_{PWV}(i), \quad (1)$$

where i represents a (well-characterised) temperate site. The application of this relation with the atmospheric parameters of

[1] Seeing above the turbulent ground layer.

[2] Dome C is even colder during winter, with an average ground temperature of −65 °C (208 K).

Table 1. Water vapour seeing at three astronomical sites. The Fried parameter r_0 is given at 500 nm, adapted from the values of Racine (2005). References for the *PWV* data are given in the last column. The standard deviation of water vapour seeing at Dome C is deduced from the data at Cerro Paranal and Mauna Kea following Eq. (1). Water vapour seeing was measured on a baseline of 66 m (resp. 100 m) at Paranal (resp. Mauna Kea), and we assume that our estimate at Dome C is valid for a similar range of baseline lengths.

Site	r_0	$\langle PWV \rangle$	σ_{PWV}	References
Cerro Paranal	14.5 cm	3 mm	27 μm	Meisner & Le Poole (2003)
Mauna Kea	17.8 cm	1.6 mm	11 μm	Colavita et al. (2004)
Dome C	38.2 cm	0.25 mm	1 μm	Bussmann et al. (2005)

either Cerro Paranal or Mauna Kea taken as a reference gives very similar estimates of 1.0 and 0.91 μm for σ_{PWV} at Dome C (see Table 1), using an average *PWV* content of 250 μm for Dome C. For this calculation, we assumed a seeing of 0.″27, which is valid only above 30 m (Lawrence et al. 2004). Using this value is recommended in the present case for two reasons: on one hand, telescopes are contemplated to be placed above the turbulent ground layer, and on the other hand, the study of Bussmann et al. (2005) shows that most of the *PWV* is concentrated between 200 m and 2 km above the ground, so that water vapour seeing is suspected to be only weakly affected by the ground layer.

3.3. Atmospheric transmission and sky brightness

Another benefit from the low water vapour content is to widen and improve the overall transmission of the infrared atmospheric windows. Lawrence (2004) shows that the *K* band is extended up to 2.5 μm and the *L* band from 2.9 to 4.2 μm. The transmission of the *M* band around 5 μm is also significantly improved.

The infrared sky brightness is also partially determined by the water vapour content, which affects its wavelength-dependent emissivity factor. The other parameter influencing the sky emission is its effective temperature, which depends on the altitude of the main opacity layer at a given wavelength. The effective temperature above South Pole has been measured by Chamberlain et al. (2000) in the mid-infrared, with values ranging from 210 K to 239 K depending on wavelength. Most of the winter sky background emission is in fact assumed to emanate from an atmospheric layer just above the temperature inversion layer, located between 50 and 200 m at Dome C (Chamberlain et al. 2000; Lawrence 2004). The atmospheric temperature at this altitude is about 230 K in wintertime (Agabi et al. 2006). As a result of both low temperature and low emissivity, the sky background is exceptionally low in Antarctica. The measurements obtained at South Pole show that is it reduced by a factor ranging between 10 and 100 in the infrared domain with respect to temperate sites. The largest gain in sensitivity for astronomical observations is expected to arise in the *K*, *L* and *M* bands. It is estimated that 1-m class telescopes at Dome C would reach almost the same sensitivity as 8-m class telescopes at a temperate site at these wavelengths.

The atmospheric parameters discussed in this section are summarised in Table 2.

Table 2. Atmospheric parameters adopted for the performance simulation of ALADDIN at Dome C, assuming that the instrument is located about 30 m above the ground level. The equivalent wind speed is the wind speed integrated across the whole turbulence profile (above 30 m).

Atmospheric parameters	
Fried parameter r_0 at 500 nm	38 cm
Equivalent seeing	0.″27
Coherence time τ_0	7.9 ms
Equivalent wind speed	15 m/s
Outer scale $L_{\rm out}$	100 m
Sky temperature	230 K
Ambient temperature at h = 30 m	230 K
Mean *PWV*	250 μm
rms *PWV*	1 μm
Pressure	640 mbar

4. The ALADDIN nulling interferometer concept

To provide plausible inputs in terms of instrumental parameters for the performance simulation, a conceptual design is needed for our Antarctic nulling interferometer. The main design guidelines that have been adopted are the minimisation of the number of open air reflections, the preservation of the full symmetry between the two beams and the optimisation of the range of baselines for typical Darwin target stars. Another critical guideline to benefit from the outstanding free air seeing is to place the instrument above the boundary layer (i.e., about 30 m above the ground at Dome C). The following sections describe a practical concept of a nulling interferometer dedicated to exozodiacal disc detection, which follows these recommendations without pretending to be optimal. This concept is referred to as ALADDIN, the Antarctic *L*-band Astrophysics Discovery Demonstrator for Interferometric Nulling.

4.1. The interferometric infrastructure

The concept proposed here consists in a 40 m long rotating truss installed on top of a 30 m tower, and on which are placed two moveable siderostats feeding off-axis telescopes (Fig. 1). Such a design has two main advantages: first, thanks to the moveable siderostats, the baseline length can be optimised to the observed target and second, thanks to the rotating truss, the baseline can always be chosen perpendicular to the line of sight so that neither long delay lines nor dispersion correctors are needed. Moreover, polarisation issues, which are especially harmful in nulling interferometry (Serabyn & Colavita 2001), are mitigated by this fully symmetric design. The available baseline lengths range from 4 to 30 m and provide a maximum angular resolution of 10 mas in the *L* band. This is largely sufficient to study the habitable zones around Darwin/TPF-I candidate targets, since they are typically separated by a few tens of milliarcseconds from their parent star (Kaltenegger et al. 2006).

For the baseline version of the ALADDIN design shown in Fig. 1, the diameter of the siderostats has been set to 1 m, which is expected to provide similar performance to 8-m class telescopes at a temperate site. Only five reflections are required to lead the light from the sky down to the instrument, which is accommodated under the rotating truss, at the rotation centre. All relay mirrors are at ambient temperature, i.e., about 230 K at that altitude during wintertime (Agabi et al. 2006). Note that an

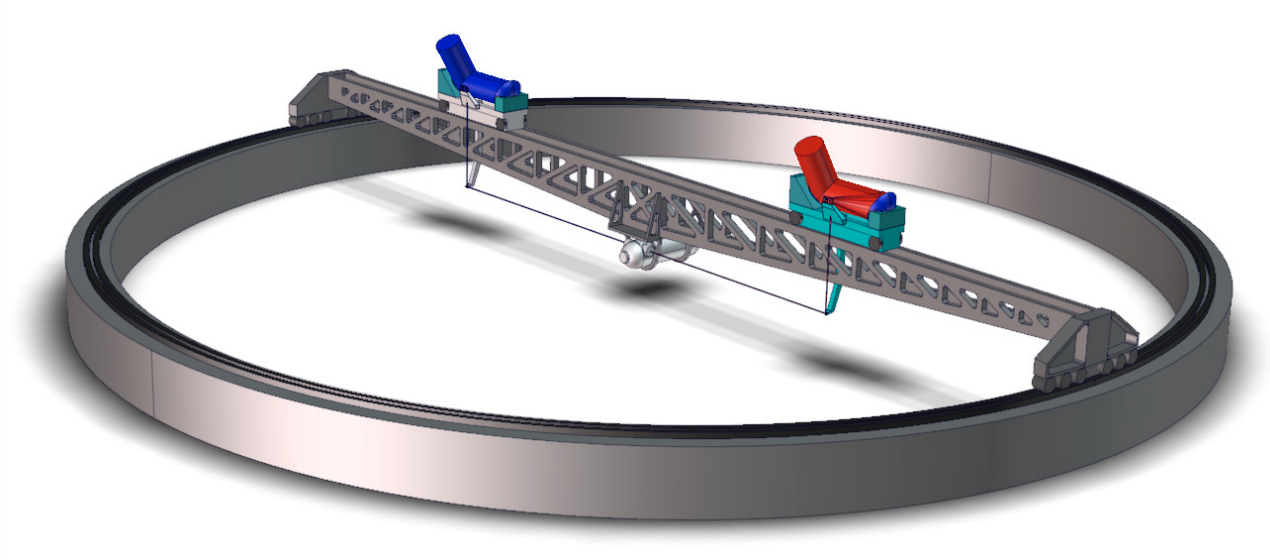

Fig. 1. Overview of the ALADDIN infrastructure. A 40-m rotating truss bearing the siderostats is mounted on a 30-m high structure (not represented). The light beams collected by the two siderostats are fed into off-axis telescopes and routed towards the nulling instrument cryostat by fixed relay optics (only five reflections outside the cryostat).

alternative design, where the instrument is placed on the ground, was introduced earlier (Barillot et al. 2006). In the latter version the cryostat does not need to be rotated with the truss and remains fully static, at the cost of a more complex optical train which enables symmetric de-rotation of the beams and preservation of the polarisation. The harmful influence of ground-layer seeing is then mitigated by propagating compressed beams about 40 mm in diameter, i.e., smaller than the typical Fried parameter in the ground layer.

4.2. The nulling instrument

The ALADDIN interferometer feeds a nulling instrument whose design is directly inherited from GENIE, a nulling instrument originally designed to be installed at ESO's Very Large Telescope Interferometer (VLTI) on top of Cerro Paranal. Using a common base design has the advantage of improving the comparative value of the performance simulations. Indeed, ALADDIN is foreseen to operate in the same wavelength regime, the L band (ranging from 2.9 to 4.2 μm at Dome C), which is very appropriate to investigate the inner region of extrasolar zodiacal discs. The whole nulling instrument is assumed to be enclosed in a cryostat, in order to improve its overall stability and to mitigate the influence of temperature variations between seasons at the ground level (the mean temperature during the austral summer is about 40 °C higher than during winter, while the instrument should be usable during the whole year). The lower temperature of the optics inside the cryostat (77 K) also further decreases the background emission produced by the instrument. Since (as is shown below) two subsystems needed for GENIE are no longer needed for the Antarctic version, the instrument is expected to be smaller and therefore easier to enclose into a cryostat.

The ALADDIN instrument comprises the same basic functionalities as GENIE (fringe tracking, tip-tilt correction, phase shifting, beam combination, modal filtering, spectral dispersion and detection), except for two critical control loops that are not needed any more. As demonstrated in Sect. 5, ALADDIN can on the one hand be operated without any dispersion correction

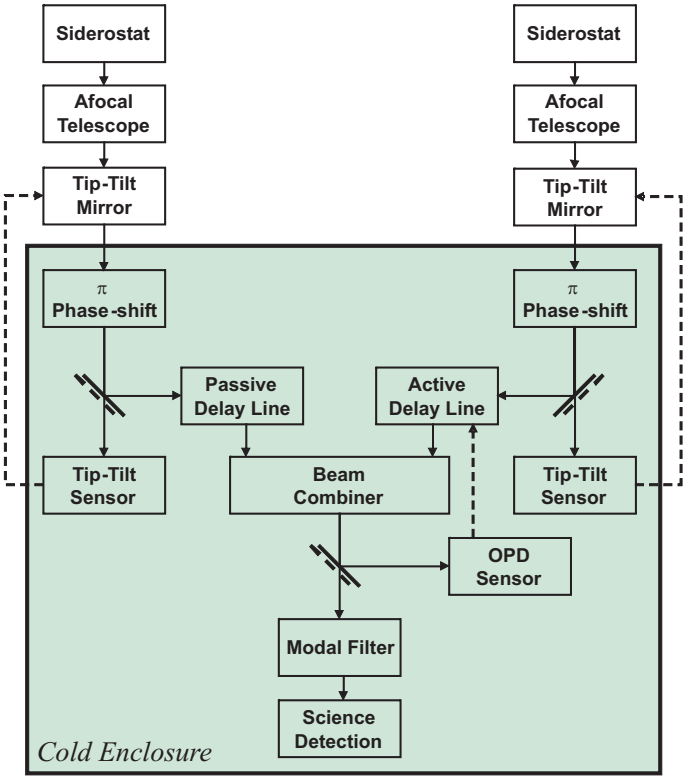

Fig. 2. Block diagram of the ALADDIN optical architecture. Feed-back signals driving the control of the tip-tilt and OPD parameters are shown in dashed lines. The entrance windows of the cold enclosure are not represented, for simplicity.

thanks to the rotating baseline and to the very low water vapour seeing, provided that the observing waveband is restricted to the 3.1–4.1 μm region, while on the other hand, real-time intensity control is not required any more since the size of the collectors is significantly smaller than the Fried parameter in the L band ($r_{0,L} \simeq 4$ m). A block diagram of the optical path and control system of ALADDIN is shown in Fig. 2. Most optical functions

are kept at low temperature inside a vacuum enclosure. The optical arrangement has been significantly simplified with respect to the original VLTI/GENIE design:

– The two-mirror afocal telescopes are off-axis. Thanks to the narrow field-of-view, high wavefront quality is expected.
– Tip-tilt correction is performed at the level of the collecting telescopes assemblies, so that the optical paths downstream are kept identical whatever the baseline and orientations of the siderostats and structural beam.
– The achromatic π phase-shift is achieved geometrically, by means of opposite periscopes.
– The beam splitters shown in Fig. 2 are actually dichroic beam splitters, which separate the signal between the science wave band and the tip-tilt and OPD sensing wave bands.
– Optical delay lines are of the short stroke/high accuracy kind, since long stroke is not necessary in the rotating beam architecture. Their design is expected to be greatly simplified with respect to usual delay lines: one-stage actuators based on linear piezoelectric motors translating a small and light plane mirror are expected to be sufficient.
– The preferred beam combiner arrangement is the Modified Mach-Zehnder (MMZ, Serabyn & Colavita 2001).
– The modal filter is a single-mode optical fibre. Fluoride glass fibres are appropriate for ALADDIN's science wavelengths.
– OPD detection may be achieved downstream the beam combiner, by means of an ABCD algorithm, provided that one of the two nulled outputs of the MMZ receives a $\pi/2$ phase shift. Alternately, the separation between OPD sensor and science bands may be implemented upstream the beam combiner and a second beam combiner accommodated for the OPD measurement. The latter option, which was the baseline for the GENIE instrument, has been used for performance estimation to provide a fair comparison with GENIE.

The control system involves three control loops only, respectively dedicated to the stabilisation of one OPD and two tip-tilt parameters. They are expected to be operated at lower repetition frequencies than at a temperate site thanks to the slowness of atmospheric turbulence, which represents a significant simplification. The control loops are based on conventional and separated PID controllers involving separated sensors and actuators. The location of the tip-tilt mirrors in the output pupil of the telescopes ensures proper uncoupling between tip-tilt actuation and OPD.

5. Performance study at Dome C

In order to evaluate the performance of ALADDIN, we use the GENIE simulation software (GENIEsim), which performs end-to-end simulations of ground-based nulling interferometers with a system-based architecture. All the building blocks and physical processes included in GENIEsim are described in detail in Paper I. They include the simulation of astronomical sources (star, circumstellar disc, planets, background emission), atmospheric turbulence (piston, longitudinal dispersion, wavefront errors, scintillation), as well as a realistic implementation of closed-loop compensation of atmospheric effects by means of a fringe tracking system and of a wavefront correction system. The output of the simulator basically consists in time series of photo-electrons recorded by the detector at the two outputs of the nulling beam combiner (constructive and destructive outputs). Various information on the sub-systems are also available on output for diagnostic. Routines dedicated to the post-processing of nulling data are also included, as described in Paper I. GENIEsim is written in the IDL language. It has been originally designed to simulate the GENIE instrument at the VLTI interferometer, and has been extensively validated in that context either by comparison with on-sky data when available (e.g., MACAO and STRAP for adaptive optics, FINITO for fringe tracking) or by comparison with performance estimations carried out by industrial partners during the GENIE phase A study.

Table 3. Summary of the instrumental parameters assumed for the performance simulation of ALADDIN. The throughput and emissivity are directly computed from the baseline instrumental design, which is based on a simplified version of the GENIE instrument.

Instrumental parameters	
Baselines	4–30 m
Telescope diameter	1 m
Number of warm optics	5
Warm optics temperature	230 K
Warm throughput	80%
Warm emissivity	20%
Number of cold optics	15
Cryogenic temperature	77 K
Cold throughput	10%
Science waveband	3.1–4.1 μm (L)
Fringe sensing waveband	2.0–2.4 μm (K)
Tip-tilt sensing waveband	1.15–1.3 μm (J)

Thanks to the versatility of the simulator, only a few input parameters have to be changed to switch from the original configuration (GENIE at Cerro Paranal) to ALADDIN at Dome C. These changes include the atmospheric transmission (Lawrence 2004), as well as the atmospheric and instrumental parameters listed in Tables 2 and 3. It must be noted that the ALADDIN performance can be modelled with greater confidence than in the case of GENIE as it does not rely on the nominal performance of an external system such as the VLTI. Furthermore, the performance should remain similar across most of the Antarctic plateau, as free air seeing is not expected to change drastically for sites located within the polar vortex. The only requirement is then to adapt the height of the structure on which the instrument is placed. In this regard, Dome C might not be the best possible site, as the boundary layer is suspected to be about 10 m thinner at Dome F (Swain & Gallée 2006b).

As in the case of GENIE, the performance is measured in terms of sensitivity to faint exozodiacal dust clouds. We assume that these dust clouds follow the same density and temperature distribution as in the solar system (Kelsall et al. 1998), except for a global density scaling factor. To account for this, we introduce the unit *zodi*, which corresponds to the global dust density in our local zodiacal cloud.

5.1. Control loop performance

Because dispersion and intensity control loops are not expected to be required in the case of ALADDIN, we have disabled these two loops in the GENIEsim software when simulating the residual atmospheric turbulence at beam combination. The simulation results are presented in Table 4, where the absence of dispersion and intensity control is represented by a 0 Hz repetition frequency. For these simulations, we have used two different assumptions on the atmospheric turbulence characteristics. The *worst case scenario* does not take into account the effect of pupil averaging, which is expected to reduce the power spectral density (PSD) of piston and dispersion at high frequencies

Table 4. Control loop performance and optimum repetition frequencies (0 Hz means that no control loop is used) as simulated on a 100 s observation sequence, for the GENIE instrument working on the 8-m Unit Telescopes (UT) at the VLTI (results taken from Paper I) and the ALADDIN instrument at Dome C. The observations are carried out in the *L* band for a Sun-like G2V star located at 20 pc using either the 47-m UT2-UT3 baseline at the VLTI (waveband: 3.5–4.1 μm) or a baseline length of 20 m for ALADDIN (waveband: 3.1–4.1 μm). The goal performance for exozodiacal disc detection discussed in Paper I appears in the last column. The total null is the mean nulling ratio including both the geometric and instrumental leakage contributions. The last line gives the standard deviation of the instrumental nulling ratio for this 100 s sequence (note that we give here the standard deviation of the mean instrumental nulling ratio computed on the whole time sequence, which is more representative than the frame-to-frame deviation presented in Paper I).

	GENIE – UT		ALADDIN		
	Worst case	Best case	Worst case	Best case	Goal
Piston	17 nm @ 20 kHz	6.2 nm @ 13 kHz	14 nm @ 3 kHz	10 nm @ 2 kHz	<4 nm
Inter-band disp.	17 nm @ 200 Hz	4.4 nm @ 300 Hz	7.0 nm @ 0 Hz	7.0 nm @ 0 Hz	<4 nm
Intra-band disp.	4.1 nm @ 200 Hz	1.0 nm @ 300 Hz	7.4 nm @ 0 Hz	7.4 nm @ 0 Hz	<4 nm
Tip-tilt	11 mas @ 1 kHz	11 mas @ 1 kHz	9 mas @ 1 kHz	9 mas @ 1 kHz	(see intensity)
Intensity mismatch	4% @ 1 kHz	4% @ 1 kHz	1.2% @ 0 Hz	1.2% @ 0 Hz	<1%
Total null	9.7×10^{-4}	6.2×10^{-4}	2.9×10^{-4}	2.2×10^{-4}	f(baseline)
Instrumental null	5.0×10^{-4}	1.5×10^{-4}	2.0×10^{-4}	1.3×10^{-4}	10^{-5}
rms null	4.5×10^{-6}	2.0×10^{-6}	5.0×10^{-6}	3.5×10^{-6}	10^{-5}

(Conan et al. 1995). This scenario thereby assumes a logarithmic slope of $-8/3$ at high frequencies for the PSD of these two quantities. Conversely, the *best case scenario* takes into account the effect of pupil averaging at high frequencies where it produces a $-17/3$ logarithmic slope. The rationale for introducing the worst-case scenario is that the $-17/3$ slope has never been observed to our best knowledge (most probably due to instrumental limitations), while spurious instrumental effects might potentially increase the high-frequency content of piston. It must be noted that the PSDs of higher order Zernike modes (tilt and above) remain the same in both scenarios and take into account pupil averaging.

The results listed in Table 4 confirm that two critical control loops (dispersion and intensity control) are not required any more: the input atmospheric perturbations for these two quantities are either well below other contributions (e.g., piston) or marginally compliant with the goal performance taken from Paper I[3]. A second important conclusion is that, in order to reach a residual piston similar to that of GENIE, fringe tracking can be carried out at a much lower frequency (about 3 kHz instead of 20 kHz). The technical feasibility of the instrument directly benefits from these two features. Finally, it must be noted that the two models for atmospheric turbulence provide similar results. There are two reasons for this: the actual shape of the power spectral density has no influence on the global fluctuation of the quantities that are not subject to real-time control, and the cut-off frequency at which the effect of pupil averaging becomes important is significantly higher than in the case of GENIE due to the reduced pupil diameter (see Paper I).

Despite its smaller collecting area, the overall performance of ALADDIN in terms of instrumental null is slightly improved with respect to GENIE's, by a factor up to 2.5 in the worst-case scenario. However, the mean instrumental nulling ratio achieved by ALADDIN is still a factor ~10 above the performance required to detect 20-zodi discs without calibrating the instrumental response. This shows that, as in the case of GENIE, the calibration of instrumental stellar leakage will be mandatory to approach the goal sensitivity of 20 zodi.

[3] Note that the strength of dispersion decreases for shorter baselines, and is only about 3 nm rms for a 4-m baseline.

5.2. Estimated sensitivity

Using the parameters of Tables 2 and 3, we have simulated the detection performance of ALADDIN for exozodiacal discs. The simulations take into account the same calibration procedures as discussed in Paper I in the context of GENIE, i.e., background subtraction, geometric leakage calibration and instrumental leakage calibration. Four hypothetic targets, representative of the Darwin star catalogue, have been chosen for this performance study: a K0V at 5 pc, a G5V at 10 pc, a G0V at 20 pc and a G0V at 30 pc. The integration time has been fixed to 30 min as in the case of GENIE. Unless specified, we have assumed a typical uncertainty $\Delta\theta_*$ of 1% on the diameters of the target stars (see Paper I) and we have used the worst case scenario for atmospheric turbulence with the $-8/3$ logarithmic slope of the power spectra at high frequencies. As demonstrated in Table 4, using the best case scenario would not significantly change the final results.

In Fig. 3, we present the results of the simulations in terms of detectable exozodiacal density level as a function of baseline length. As in Paper I, the threshold for detection is set at a global signal-to-noise of 5, including the residuals from background subtraction and from geometric and instrumental stellar leakage calibration. Figure 3 shows that the optimum baseline for studying typical Darwin target stars is comprised between about 4 and 40 m, which closely matches the baseline range offered by ALADDIN. With its 1 m class telescopes, ALADDIN significantly outperforms GENIE for the same integration time in the case of nearby targets (see Table 6 for a thorough comparison). This fact is not only due to the exceptional atmospheric conditions, but also to the optimisation of ALADDIN both regarding the available baselines and the instrumental design.

To check the relevance of ALADDIN in the context of the Darwin preparatory science, it is useful to compare the angular resolution provided by the optimum baseline length with respect to the position of the habitable zone for the various targets, because Darwin will be most sensitive to dust located in that particular zone where it will search for Earth-like planets. According to Kasting et al. (1993), the position of the habitable zone expressed in AU is given in good approximation by the following equation:

$$r_{\mathrm{HZ}} = \left(\frac{T_\star}{T_\odot}\right)^2 \frac{R_\star}{R_\odot}, \tag{2}$$

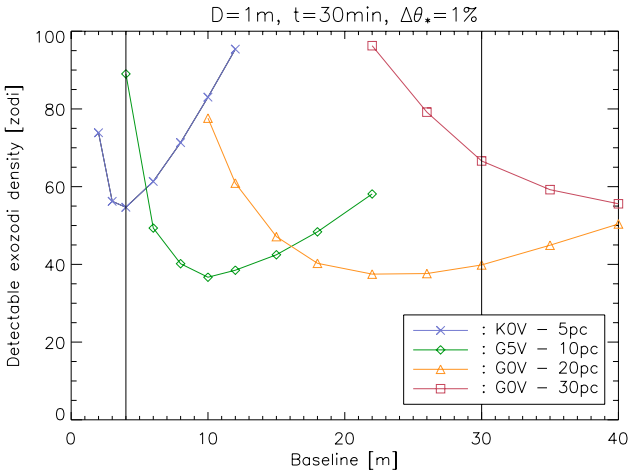

Fig. 3. Simulated performance of ALADDIN in terms of exozodiacal disc detection for four typical Darwin targets. The baseline design for ALADDIN has been used (see Table 3), assuming an integration time of 30 min, an uncertainty of 1% on the knowledge of the stellar angular diameter, and using the worst-case scenario for atmospheric turbulence (see text). The two vertical lines indicate the baseline range proposed for the ALADDIN conceptual design.

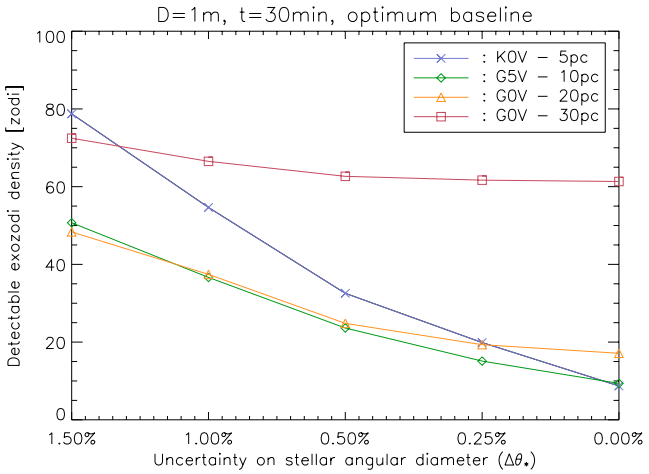

Fig. 4. Simulated performance of ALADDIN in terms of exozodiacal disc detection for various assumptions on the uncertainty on the stellar angular diameters.

Table 5. Comparison of the angular resolution provided by the optimum ALADDIN baseline length ($4 \leq b \leq 30$ m) with the characteristic position of the habitable zone of the target systems.

	Optimum baseline	Ang. resol. ($\lambda/2b$)	Position HZ ($r_{\rm HZ}/d$)
K0V 5 pc	4 m	93 mas	135 mas
G5V 10 pc	10 m	37 mas	85 mas
G0V 20 pc	24 m	15 mas	58 mas
G0V 30 pc	30 m	12 mas	39 mas

which yields 0.68, 0.85 and 1.16 AU for a K0V, a G5V and a G0V star respectively. The angular distance of the habitable zone to its parent star is compared to the angular resolution of ALADDIN in Table 5. The first bright fringe of the optimised nulling interferometer always falls between the star and the habitable zone, and the associated angular resolution is compatible with the study of this most important region of the exozodiacal disc. This also validates a posteriori the choice of the L band for the study of exozodiacal dust around the Darwin target stars.

5.3. Calibration of stellar angular diameters

An important parameter influencing the performance of a nulling interferometer is the uncertainty on the angular diameter of the target star ($\Delta\theta_\star$). It is the main contributor to the quality of calibration not only for geometric stellar leakage but also for instrumental stellar leakage, which relies on the estimation of the instrumental nulling ratio on a well-known calibration star. In Fig. 4, we investigate the influence of this $\Delta\theta_\star$ parameter on the ALADDIN sensitivity. The baseline length is optimised in each case within the specified range (4–30 m). This simulation shows that, similarly to the GENIE case, an improved accuracy on stellar diameters would largely improve the detection capabilities of ALADDIN.

The very good sensitivity obtained for a perfect knowledge of the stellar diameter gives an idea of the gain that could be achieved by using more elaborate nulling configurations that are almost insensitive to stellar leakage. An example of such a configuration is the Degenerate Angel Cross (Mennesson et al. 2005), which uses three aligned telescopes to provide a central transmission proportional to the fourth power of the angular distance to the optical axis (θ^4) instead of the second power (θ^2) for a two-telescope Bracewell interferometer. The use of phase chopping with multi-telescope configurations would have almost the same effect, as geometric stellar leakage would then be removed by the chopping process. Figure 4 shows that an advanced nulling interferometer at Dome C should be capable of reaching a sensitivity ranging between 10 and 20 zodi around most of the Darwin targets. Multi-telescope configurations are however not contemplated in the context of ALADDIN, for which simplicity is strongly advocated.

Table 6. Comparison of the GENIE and ALADDIN performance expressed in detectable exozodiacal disc densities as compared to the solar zodiacal disc. Four different levels of uncertainty have been assumed on the angular diameter of the target stars. The simulations are performed in the L band, which extends from 3.5 to 4.1 μm in the case of GENIE and from 3.1 to 4.1 μm in the case of ALADDIN. An integration time of 30 min is assumed in all cases.

Star	0.25%	0.5%	1%	1.5%	Instrument
K0V – 5 pc	72	90	125	154	GENIE – AT
	114	227	455	682	GENIE – UT
	20	33	55	79	ALADDIN
G5V – 10 pc	111	130	154	176	GENIE – AT
	30	59	117	176	GENIE – UT
	15	24	37	51	ALADDIN
G0V – 20 pc	255	261	278	297	GENIE – AT
	21	29	50	73	GENIE – UT
	19	25	37	48	ALADDIN
G0V – 30 pc	575	585	604	615	GENIE – AT
	36	46	59	71	GENIE – UT
	62	63	67	72	ALADDIN

Table 6 compares the expected sensitivity of ALADDIN, operated on 1-m telescopes, with that of GENIE on either 8-m Unit Telescopes or 1.8-m Auxiliary Telescopes at the VLTI, using various assumptions on the stellar diameter knowledge. A significant gain (up to a factor 4) is obtained with ALADDIN, except in the case of the G0V at 30 pc where the 8-m telescopes are providing a more suited collecting area. The gain with ALADDIN is all the larger when the target star is closer, because the use

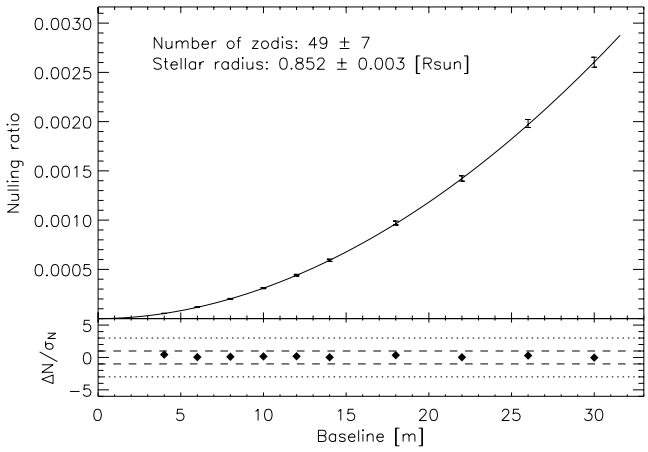

Fig. 5. Simultaneous fit of the stellar radius and the exozodiacal density level using ten 30-min observations of a K0V star at 5 pc (actual radius of 0.85 $R_\odot$), surrounded by a 50-zodi disc. The nulling ratio is computed as the ratio between the destructive and constructive outputs of the beam combiner. The contribution of instrumental stellar leakage to the nulling ratio has been subtracted from this data using the same procedure than elaborated for GENIE: the observation of a calibration target of similar type and distance, but without circumstellar material.

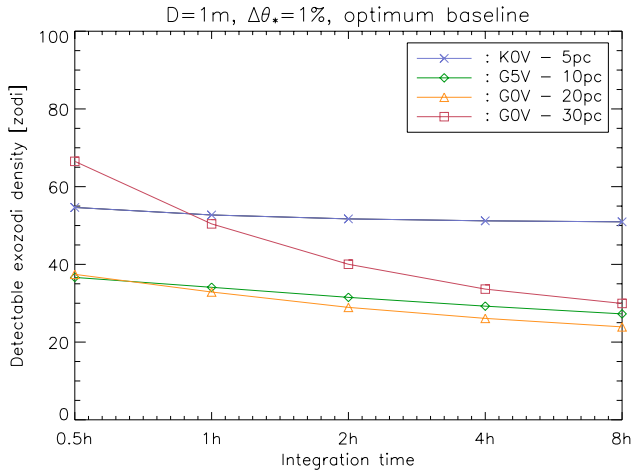

Fig. 6. Simulated performance of ALADDIN in terms of exozodiacal disc detection for increasing integration times.

of short baselines is crucial for stars with relatively large angular diameters ($\gtrsim$1 mas). As obvious from Table 6, an accurate knowledge of the stellar angular diameter (<0.5%) at the observing wavelength is mandatory to reach our goal sensitivity of 20 zodi.

Angular diameters in the L band are however currently not well constrained, due to the lack of actual measurements. Furthermore, it is not guaranteed that an interferometer will operate in this band in a near future to provide angular diameter measurements with the required accuracy, while extrapolating stellar models from the visible or near-infrared (H, K bands) towards the L band is not straightforward (see Paper I). An integrated concept as ALADDIN presents a significant advantage in this respect, as the continuous range of available baselines can be used to fit the stellar angular diameter simultaneously with the exozodiacal disc parameters. This procedure is illustrated in Fig. 5, where we have simulated ten 30-min observations of a K0V star at 5 pc surrounded by a 50-zodi disc, using ten baseline lengths ranging between 4 and 30 m. All standard calibrations have been applied in these observations, except for the calibration of the geometric stellar leakage (which is actually the main contributor to the observed nulling ratio). The simultaneous fit of the stellar radius and the exozodiacal dust density level provides encouraging results, and confirms that the a priori knowledge of the stellar radius is not required if a sufficient baseline coverage is used.

5.4. Influence of integration time

Another advantage of the ALADDIN concept is its ability to perform very long on-source integrations. The interferometer is assumed to be continuously operated during the long winter night, but also during the equinox twilight and the summer day thanks to the low sky temperature in all seasons and to the very low aerosol and dust content in the atmosphere (coronal sky). The summertime performance will of course be somewhat degraded due to the unavoidable stray light in the instrument and to the higher temperature of the sky and optical train, which produces a larger background emission. Long integrations are also enabled by the fact that ALADDIN would be dedicated to the survey of exozodiacal discs, while an instrument like GENIE would have to compete with other instruments at the VLT (especially when using the 8-m Unit Telescopes). Therefore, it makes sense to investigate the gain in sensitivity that can be achieved by longer integrations. The computation of this gain is not trivial, as all the noise sources do not have the same temporal behaviour. For instance, shot noise, detector noise and instability noise (to the first order) have the classical $t^{1/2}$ dependence, while the imperfect calibration of geometric and instrumental stellar leakage is proportional to time (it actually acts as a bias).

In Fig. 6, we simulate the sensitivity of ALADDIN as a function of integration time. Because increasing the integration time does not improve the accuracy of both geometric and instrumental stellar leakage calibration, which are among of the main contributors to the noise budget (especially for very nearby stars), the overall performance does not largely improve for long exposures (except for the fainter targets, for which sensitivity is background-limited). It must still be noted that a sensitivity ranging between 20 and 30 zodis is within reach after 8 h of integration for the farthest targets.

A side effect of increasing the integration time is that the optimum baseline is decreased. Indeed, shorter baselines allow for less exozodiacal light to make it through the transmission pattern, but also for a better cancellation of the stellar light. The result is an improved signal-to-noise ratio regarding stellar leakage calibration, while the relative increase of the shot noise contribution with respect to the transmitted exozodiacal signal is compensated by the longer integration time. For instance, in the case of a G0V star at 20 pc, the optimum baseline decreases from 24 m for a 30 min integration to 12 m for an 8 h integration. Reducing the optimum baseline is favourable to the global feasibility of the concept, as it reduces the required size of the truss supporting the siderostats.

5.5. Influence of pupil diameter

Finally, in order to choose the most appropriate diameter for the ALADDIN siderostats, we study the influence of the collecting area on the sensitivity of the instrument. To keep the system architecture unchanged, we restrict the pupil diameter to 2 m at

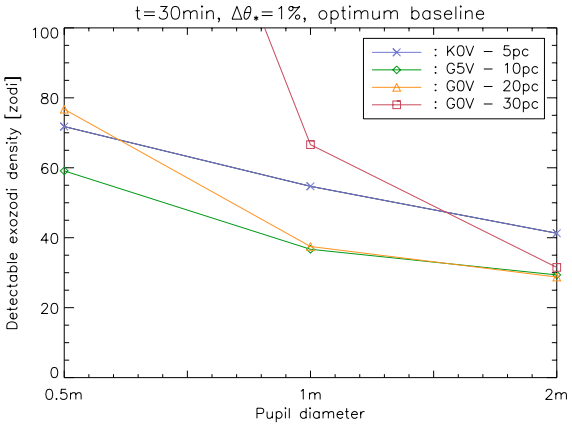

Fig. 7. Simulated performance of ALADDIN in terms of exozodiacal disc detection for three different pupil diameters (50 cm, 1 m and 2 m).

most, since larger pupils would become comparable to the size of turbulent cells above the boundary layer (about 4 m in the L band) and would therefore require either adaptive optics or additional intensity control to be implemented.

Figure 7 shows the simulated performance of ALADDIN for three different sizes of the siderostats. By increasing the diameter from 0.5 m to 1 m, the performance improves by a factor ranging from 25% to 75%, while a typical gain between 25% and 50% is observed when increasing the telescope size from 1 m to 2 m. The G0V star at 30 pc shows the most significant improvement as a function of pupil size, due to its faintness (shot noise from the background emission is dominant for such a faint star). It must be noted that the performance of ALADDIN with 50-cm collectors is still better than that of GENIE at the VLTI for the two closest targets. Reducing the size of the siderostats could thus make sense if the feasibility of the project was found to be jeopardised by the requirement to put 1-m siderostats on a 40-m truss located 30 m above the ground. Increasing the integration times by a factor about 4 would then be required to achieve similar performance as with 1-m collectors. A beneficial side-effect of increasing the integration time will be to reduce the optimum baselines down to an acceptable length, because 50-cm siderostats are associated with optimum baselines typically twice as large as for the original 1-m collectors. In practice, the final choice of the pupil diameter will result from a trade-off between feasibility, performance, integration time and available baselines.

6. Site impact on performance

In this section, we estimate the gain in performance that is actually related to the outstanding observing conditions above the boundary layer on the Antarctic plateau (and not to the optimised instrumental design). For that purpose, we simulate the performance of ALADDIN at two other locations: first on the ground at Dome C (below the boundary layer) and then at Cerro Paranal. In the first case, we use the ground-level wintertime seeing conditions recently reported at Dome C by Agabi et al. (2006): a median seeing of 1.″9 (i.e., a Fried parameter of 5.4 cm at 500 nm) and a coherence time of about 2.9 msec (i.e., equivalent wind speed of 5.8 m/s). In the second case, we use the standard atmospheric conditions of Cerro Paranal already presented in Paper I.

6.1. Ground-level performance at Dome C

One of the main limitations of ground-level observations comes from the fact that the Fried parameter in the L band (~57 cm) becomes smaller than the size of the apertures, so that multiple speckles are formed in the image plane. Assuming only tip-tilt control at 1 kHz, which provides a residual tip-tilt of about 15 mas, the typical fluctuations of the relative intensity mismatch between the two beams after modal filtering would be about 18%. This is much too large to ensure a high and stable instrumental nulling ratio, and the use of adaptive optics (or of an intensity matching device) is therefore required to stabilise the injection into the single mode waveguides. Another limitation comes from the increased strength of the piston effect. Assuming fringe tracking to be performed at a maximum frequency of 10 kHz, the residual OPD would range between 15 and 35 nm rms depending on the target star. Here again, the stability of the nulling ratio would be significantly degraded with respect to the baseline ALADDIN concept. On the contrary, longitudinal dispersion is not expected to increase very significantly since the precipitable water vapour content of the first 30 m of the atmosphere is relatively small due to the very low temperature right above the ice.

Taking all these effects into account, the instability of the nulling ratio (*instability noise*) would become the main source of noise in the budget of a ground-level ALADDIN. The simulations performed with GENIEsim show that the sensitivity in the case of a G0V star located at 20 pc would only be about 200 zodi instead of 37 zodi for the original ALADDIN concept on top of a 30-m tower. In order to match the baseline ALADDIN performance with a ground-level instrument, higher repetition frequencies would be required for piston and tip-tilt control (both about 6 kHz), while adaptive optics (or intensity control) should be used to stabilise the injection efficiency into the waveguides. Dispersion control might also be required. Preliminary estimations show that deformable mirrors using 20×20 actuators at a repetition frequency around 1 kHz would be required to reduce the intensity fluctuations down to 1%. In that case, a sensitivity around 50 zodi would be reachable for a G0V star at 20 pc.

Obviously, placing the instrument above the ground layer is recommended to obtain a significant gain on both the performance and feasibility aspects with respect to an instrument installed at a temperate site such as Cerro Paranal.

6.2. Ground-level performance at Cerro Paranal

To better emphasise the attractiveness of Antarctic sites in the context of high dynamic range interferometry, let us now virtually move the ALADDIN experiment to Cerro Paranal while keeping the design unchanged. Because the Fried parameter is larger at Paranal ($r_0 \sim 1.2$ m in the L band) than at the ground level at Dome C, while the coherence time is of the same order of magnitude ($\tau_0 \sim 3$ msec), the performance should be somewhat better than on the ground at Dome C. Simulations indeed show that the residual OPD is slightly improved (now between 10 and 30 nm), while the residual intensity fluctuation is significantly reduced (now about 7%, but still well above the goal of 1%).

However, two other parameters significantly degrade the situation: the large background emission and the increased *PWV* content in the atmosphere. The main effect of the former is to increase the integration time needed to reach a given sensitivity limit, while the fluctuations of the latter produce large variations of longitudinal dispersion, which can reach about 0.7 radian if they are not reduced by a real-time control loop as in the case

of GENIE (see Paper I). This corresponds to an additional OPD error of about 400 nm at the edges of the observing waveband (ranging from 3.5 to 4.1 μm in the case of Cerro Paranal). All in all, a sensitivity of about 3000 zodi is expected for a replica of ALADDIN installed at Cerro Paranal. By introducing a dispersion control loop similar to that described in Paper I and operating it at a typical frequency of 50 Hz, longitudinal dispersion could be reduced down to about 0.05 radian (30 nm), in which case the sensitivity would reach about 250 zodi. This would however significantly increase the technical complexity of the instrument, which is not desired.

7. Conclusion

In this paper, we have investigated a potential solution to a well-defined scientific need, viz. characterising the dusty environment of candidate target stars for future life-finding missions such as Darwin or TPF. In a previous study (Paper I), we have shown that an infrared nulling interferometer installed on a temperate site, such as the GENIE project at Cerro Paranal, would provide useful information on candidate targets, but (1) that its technical feasibility could be jeopardised by the requirement to design complicated control loops for mitigating the effects of atmospheric turbulence, and (2) that its sensitivity would not reach the desired level of 20 times the density of our local zodiacal cloud.

To overcome these two limitations, we propose in this paper a conceptual design for a nulling interferometer (ALADDIN) to be installed at Dome C, on the high Antarctic plateau. Based on the atmospheric turbulence measurements obtained so far at Dome C, we have updated the GENIEsim software (Paper I) to simulate the performance of such an instrument. These simulations show that, using 1-m collectors, this instrument would have an improved sensitivity with respect to GENIE working on 8-m telescopes, provided that it is placed above the turbulence boundary layer, which is about 30 m thick at Dome C. In particular, the 20-zodi sensitivity goal seems within reach for typical Darwin/TPF target stars. Moreover, the exceptional turbulence conditions above the boundary layer significantly relax the requirements on the real-time compensation of atmospheric effects, improving the feasibility of the instrument. It must also be noted that, thanks to the optimised range of adjustable baselines, the harmful influence of our imperfect knowledge of stellar angular diameters can be largely mitigated by simultaneously fitting a photospheric model and an exozodiacal disc model to the collected data, yet at the price of an increased observing time.

While we assumed the instrument would be deployed above the boundary layer at Dome C, site of the Concordia station, it might turn out that other sites on the Antarctic plateau provide simultaneously a thinner boundary layer and an improved free air seeing, and hence better performance. The final choice for the site will have to trade off the practical advantages of feasibility and performance vs. logistical support.

This paper illustrates the potential of Antarctic sites for high-angular, high-dynamic range astrophysics in the infrared domain. In the particular, well specified case of a nulling interferometer, we were able to realistically quantify the relative gain with respect to a temperate site, showing that a pair of 1 m telescopes on the plateau will perform better than a pair of 8 m telescopes at Cerro Paranal. Other applications would result in different gains, but it is clear that there are niches where the Antarctic plateau enables observations that would otherwise require access to space.

Acknowledgements. The authors are indebted to R. den Hartog and D. Defrère for their major contributions to the development of the GENIEsim software, which has been used throughout this paper. The authors also wish to thank the engineers at Thales Alenia Space that have contributed to the preliminary design of the ALADDIN instrument, as well as T. Fusco for the simulation of adaptive optics performance at Dome C. O.A. acknowledges the financial support of the Belgian National Fund for Scientific Research (FNRS) while at IAGL and of a Marie Curie Intra-European Fellowship (EIF) while at LAOG.

References

Absil, O., den Hartog, R., Gondoin, P., et al. 2006a, A&A, 448, 787
Absil, O., Di Folco, E., Mérand, A., et al. 2006b, A&A, 452, 237
Agabi, A., Aristidi, E., Azouit, M., et al. 2006, PASP, 118, 344
Aristidi, E., Agabi, A., Vernin, J., et al. 2003, A&A, 406, L19
Aristidi, E., Agabi, A., Fossat, E., et al. 2005, A&A, 444, 651
Barillot, M., Courteau, P., Absil, O., Coudé du Foresto, V., & Swain, M. 2006, in Advances in Stellar Interferometry, ed. J. D. Monnier, M. Schöller, & W. C. Danchi, 2Z–1, Proc. SPIE, 6268
Beichman, C. A., Woolf, N. J., & Lindensmith, C. A., eds. 1999, The Terrestrial Planet Finder (TPF): a NASA Origins Program to search for habitable planets (Pasadena: JPL Publication 99-3)
Beichman, C. A., Bryden, G., Stapelfeldt, K. R., et al. 2006, ApJ, 652, 1674
Bussmann, R. S., Holzapfel, W. L., & Kuo, C. L. 2005, ApJ, 622, 1343
Candidi, M., & Lori, A. 2003, Mem. Soc. Astron. It., 74, 29
Chamberlain, M. A., Ashley, M. C. B., Burton, M. G., et al. 2000, ApJ, 535, 501
Chamberlin, R. A., Lane, A. P., & Stark, A. A. 1997, ApJ, 476, 428
Colavita, M. M., Swain, M. R., Akeson, R. L., Koresko, C. D., & Hill, R. J. 2004, PASP, 116, 876
Conan, J.-M., Rousset, G., & Madec, P.-Y. 1995, J. Opt. Soc. Am. A, 12, 1559
Di Folco, E., Absil, O., Augereau, J.-C., et al. 2007, A&A, in press
Fridlund, C. V. M. 2004, Adv. Space Res., 34, 613
Gondoin, P. A., Absil, O., den Hartog, R. H., et al. 2004, in New Frontiers in Stellar Interferometry, ed. W. Traub, Proc. SPIE, 5491, 775
Kaltenegger, L., Eiroa, C., Stankov, A., & Fridlund, M. 2006, in Direct Imaging of Exoplanet: Science & Techniques, ed. C. Aimé, & F. Vakili, Proc. IAU Coll., 200, 255
Kaltenegger, L., Traub, W. A., & Jucks, K. W. 2007, ApJ, 658, 598
Kasting, J. F., Whitmire, D. P., & Reynolds, R. T. 1993, Icarus, 101, 108
Kelsall, T., Weiland, J. L., Franz, B. A., et al. 1998, ApJ, 508, 44
Lawrence, J. S. 2004, PASP, 116, 482
Lawrence, J. S., Ashley, M. C. B., Burton, M. G., et al. 2003, in Toward Other Earths: Darwin/TPF and the Search for Extrasolar Terrestrial Planets, SP-539 (ESA's Publication Division), 497
Lawrence, J. S., Ashley, M. C. B., Tokovinin, A., & Travouillon, T. 2004, Nature, 431, 278
Lay, O. P. 1997, A&AS, 122, 535
Marks, R. D. 2002, A&A, 385, 328
Marks, R. D., Vernin, J., Azouit, M., Manigault, J. F., & Clevelin, C. 1999, A&AS, 134, 161
Meisner, J. A., & Le Poole, R. S. 2003, in Proc. SPIE, 4838, Interferometry in Optical Astronomy II, ed. W. Traub, 609
Mennesson, B., Léger, A., & Ollivier, M. 2005, Icarus, 178, 570
Racine, R. 2005, PASP, 117, 401
Roddier, F. 1981, in Progress in optics, ed. E. Wolf, Vol. XIX (Amsterdam: North-Holland), 281
Serabyn, E., & Colavita, M. M. 2001, Appl. Opt., 40, 1668
Swain, M. R., & Gallée, H. 2006a, in Ground-based and Airborne Telescopes, ed. L. M. Stepp, Proc. SPIE, 6267, 1K
Swain, M. R., & Gallée, H. 2006b, PASP, 118, 1190
Travouillon, T., Ashley, M. C. B., Burton, M. G., Storey, J. W. V., & Loewenstein, R. F. 2003, A&A, 400, 1163